



DOI: 10.29026/oea.2019.190014

# Polariton lasing in InGaN quantum wells at room temperature

Jinzhaoh Wu<sup>1</sup>, Hao Long<sup>1\*</sup>, Xiaoling Shi<sup>1</sup>, Song Luo<sup>2</sup>, Zhanghai Chen<sup>2</sup>, Zhechuan Feng<sup>3</sup>, Leiying Ying<sup>1</sup>, Zhiwei Zheng<sup>1</sup> and Baoping Zhang<sup>1\*</sup>

In this paper, we report the exciton polaritons in both positive and negative detuning micro cavities based on InGaN multi-quantum wells (MQWs) and the first polariton lasing in InGaN/GaN MQWs at room temperature by utilizing a 4.5λ Fabry-Perot (F-P) cavity with double dielectric distributed Bragg reflectors (DBRs). Double thresholds corresponding respectively to polariton lasing and photonic lasing are observed along with half-width narrowing and peak blue-shifts. The threshold of polariton lasing is about half of the threshold of photonic lasing. Our results paved a substantial way for ultra-low threshold lasers and room temperature Bose-Einstein Condensate (BEC) in nitride semiconductors.

**Keywords:** exciton-polariton; polariton lasing; InGaN QWs

Wu J Z, Long H, Shi X L, Luo S, Chen Z H et al. Polariton lasing in InGaN quantum wells at room temperature. *Opto-Electron Adv* 2, 190014 (2019).

Exciton polaritons, bosonic quasi particles by strong coupling between photons and excitons, were firstly depicted by J. J. Hopfield in 1950s<sup>1</sup>. The unique physical properties of light effective mass, tunable energy dispersions and convenient detection guaranteed their extensive research in nonlinear optics, low threshold lasing, quantum vortex and superfluid<sup>2</sup>.

In contrast with conventional photonic lasing, polariton lasing results from polaritons' condensation and is promising for the super-low threshold lasing due to its coherent spontaneous emission character<sup>3-5</sup>. The polariton lasing at room temperature (RT) based on GaN<sup>6</sup>, ZnO<sup>7</sup>, and perovskite<sup>8</sup> have been demonstrated recently. Among them, GaN-based III nitride material systems are essential toward practical opto-electrical devices (LD, LED, etc.)<sup>9-11</sup>, with the ultraviolet to infrared full spectral coverage of Ga(In, Al)N alloys. In 2007, J. J. Baumberg et al. reported the first optically pumping polariton lasing in bulk GaN material<sup>6</sup>, followed by electrically injected polariton lasing in bulk GaN<sup>12</sup> by P. Bhattacharya at RT in 2014. In 2004, T. Tawara et al. observed the exciton polariton in InGaN quantum wells (QWs) at room temperature by reflectance spectrum<sup>13</sup>. In 2011, T. C. Lu et al.

successfully achieved the current injected InGaN MQWs polariton LED<sup>14</sup>. However, no polariton lasing in InGaN quantum wells has been reported yet, although the realization of InGaN based polariton lasing will be significant due to the vast application of InGaN in the solid-state lighting and lasing. Strong coupling in InGaN QWs system has been shown difficult since the large inhomogeneous broadening (due to Indium phase separation and well width fluctuation) and piezoelectrical field. In 2006 and 2014, N. Grandjean et al. theoretically anticipated that less than 46 meV inhomogeneous broadening was the prerequisite for the observation of exciton polariton lasing in InGaN QWs systems<sup>15,16</sup>. They predicted that polariton lasing may be possible by combination of low Indium content and double-sides dielectric distributed Bragg reflectors (DBRs). Previously, we achieved giant Rabi splitting energy of 130 meV by coupled QWs and superior F-P cavity ( $Q > 3500$ )<sup>17</sup>.

In this work, we reported the first room temperature polariton lasing in InGaN/GaN multi-quantum wells (MQWs) by further thinning the cavity length to 4.5λ F-P cavity structure sandwiched by two dielectric DBRs. By adjusting the cavity length, strong coupling effects were

<sup>1</sup>Department of Electronic Engineering, School of Electronic Science and Engineering (National Model Microelectronics College), Xiamen University, Xiamen 361005, China. <sup>2</sup>Surface Physics Laboratory, Department of Physics, Fudan University, Shanghai 200433, China. <sup>3</sup>School of Physical Science and Technology, Guangxi University, Nanning 530004, China.

\*Correspondence: H Long, E-mail: longhao@xmu.edu.cn; B P Zhang, E-mail: bzhang@xmu.edu.cn

Received: 23 April 2019; Accepted: 22 May 2019; Published: 20 December 2019

observed in positive and negative detuning scenarios respectively. Dual thresholds corresponding to polariton lasing and photonic lasing were clearly observed in negative detuning cavity. The nonlinear optical properties, half-width narrowing and peak blue-shifts were also confirmed. The gap between these two lasing thresholds was smaller compared with GaAs and GaN based binary crystal systems, which should be contributed to the severe inhomogeneous broadening and large negative detuning value.

Here, the studied microcavity structure (Fig.1(a)) consists of 16.5 pairs of bottom  $\text{Ti}_3\text{O}_5/\text{SiO}_2$  DBR, five periods of 4 nm  $\text{In}_{0.1}\text{Ga}_{0.9}\text{N}/4$  nm GaN MQWs active layers embedded at the antinode of the optical stationary wave (Fig.1(b)) and 13.5 pairs of top  $\text{Ti}_3\text{O}_5/\text{SiO}_2$  DBR. The fabrication process of studied microcavity was similar to our previous vertical cavity surface emitting lasers (VCSELs)<sup>18–19</sup>. The GaN layer and InGaN/GaN MQWs were grown on sapphire by metal organic vapor phase epitaxy (MOVPE), followed by the bottom DBR deposi-

tion, laser lift off of sapphire substrate, lapping and polishing of the buffer and undoped GaN layers by chemical mechanical polishing (CMP), and top DBR deposition. The thinning process of GaN material was utilized to control the cavity length and thus the detuning energy between cavity mode and exciton. The exciton ( $\sim 3.03$  eV) and corresponding LO phonon assisted ( $\sim 2.94$  eV) luminescence of InGaN MQWs were identified by photoluminescence (PL) at 15 K<sup>20–21</sup> (Figs. 1(c) and 1(d)), accompanied by another exciton ( $\sim 3.09$  eV) originated from another potential minima. The inhomogeneous half-width of 3.03 eV exciton at 15 K was 43 meV, which is the state of the art and typically larger than 5 meV in InGaN bulk<sup>22</sup> and 23 meV in GaN/AlGaIn QWs<sup>16</sup>. Elevating to room temperature, the LO replica of 2.94 eV shrunk, meanwhile the luminous bands smeared into one single asymmetric peak at 3.01 eV with a 3.06 eV shoulder on the high energy side. We investigated the polariton dispersions of InGaN/GaN MQWs by angle-resolved micro-PL (Fig. 2(a)) and micro-PL Fourier imaging (Fig. 2(b)). The radius of 355 nm pulse laser (20 kHz frequency and 3 ns pulse width) excitation spot was confined to be 2  $\mu\text{m}$ . In Fig. 2(a), the spectrums from different angles were collected by the rotation of optical fiber and lens with the angle interval of  $3^\circ$ . In Fig. 2(b), the detection range of Fourier image was defined by the numerical aperture of objective lens, corresponding to about  $\pm 48^\circ$ . Fourier images of k-space dispersion curves were recorded by CCD spectrometer under different excitation powers.

In positive detuning cavity (where the energy of cavity mode is larger than the exciton energy), two distinctive PL peaks were observed under 16 nJ/pulse excitation fluence as shown in Fig. 2(c). Keeping the exciton energy of 3.01 eV, the detuning energy at  $k_{\parallel}=0$  and Rabi splitting energy  $2\hbar\Omega$  were simulated to be 25 meV and 35 meV by the coupled harmonic oscillator model<sup>2</sup> fitting with:

$$E_{\text{LP,UP}}(k_{\parallel}) = \frac{1}{2} \left[ E_{\text{exc}} + E_{\text{cav}} \mp \sqrt{(2\hbar\Omega)^2 + (E_{\text{exc}} - E_{\text{cav}})^2} \right]. \quad (1)$$

However, in the positive detuning cavity, the lower polariton band (LPB) has large portion of exciton, which increases the mass of LPB and impedes polariton's condensation. The polariton lasing could not be observed by increasing excitation power in this sample.

For realizing polariton condensation, a negative detuning cavity was fabricated. Fig. 2(e) shows the k-space mapping of angle-resolved photoluminescence spectrum of negative detuning sample under low excitation (nominal  $\sim 70 \mu\text{W}$ ). A clear dispersion curve of LPB was observed. Whereas, unlike the positive detuning sample, the upper polariton band (UPB) was hardly identified. This phenomenon was broadly demonstrated by other similar papers<sup>8,23–26</sup>, in which the UPB could only be visible in zero or positive detuning rather than negative detuning samples. Although the effect of detuning value on the visibility of UPB still needs to be uncovered, our experimental PL conformed with the simulation results of S.

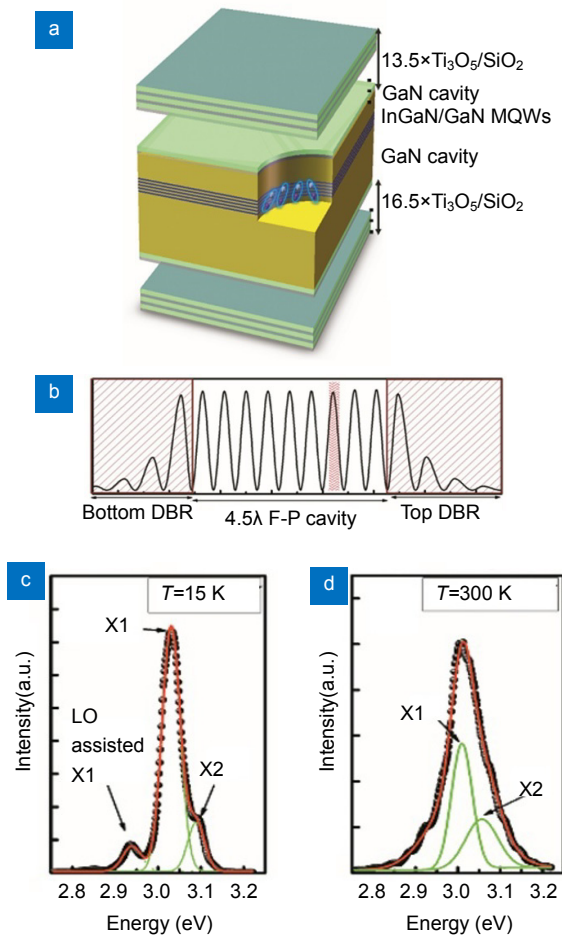


**Fig. 1** | (a) Sample structure of InGaN/GaN MQWs microcavity for strong coupling. (b) The optical field in the microcavity with MQWs placed on the antinode. (c) and (d) Photoluminescence spectrums of bare wafer at 15 K and 300 K.

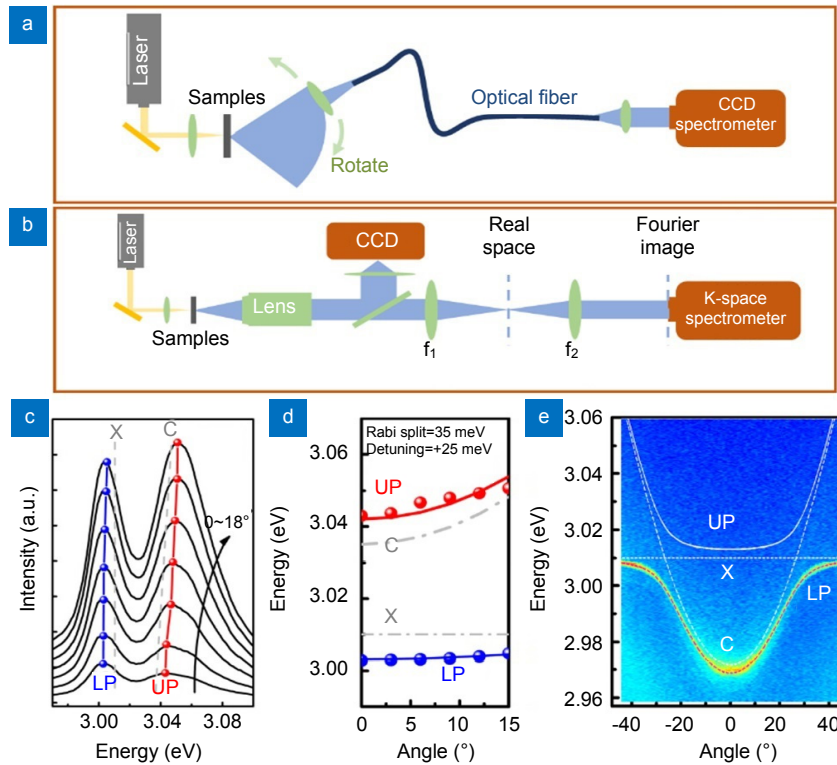


**Fig. 2 |** (a) Schematic of angle-resolved micro-PL setup. (b) Schematic of angle-resolved PL Fourier image setup. (c) The angle resolved micro-PL of positive detuning sample. (d) LPB and UPB dispersion curves fitted by coupled oscillator model. (e) The angle resolved micro-PL Fourier image of negative detuning sample.

Faure et al.<sup>25</sup>, which predicted that the UPB of GaN microcavity was damped in the negative detuning regime but well defined in positive detuning regime (Fig. 2 of Ref. <sup>25</sup>). Two unambiguous evidences were presented in the energy dispersion curve of LPB, which definitely confirmed the strong coupling between cavity photons and excitons: i) the curvature of the dispersion curve switched from parabolic to flat at large angles, which manifested the transition of photon-like polariton into exciton-like polariton; ii) keeping 3.01 eV of exciton position, the dispersion curve of polaritons and cavity photons could be theoretically fitted precisely based on the coupled harmonic oscillator model. The onset of distinctive anti-crossing between the exciton and cavity mode was observed along with the curving of LPB energy dispersion. Rabi splitting energy of 22 meV and detuning energy of -38.1 meV were obtained from the theoretical fitting.

Figure 3 shows the nonlinear properties of the integrated light output intensity, half-width and peak positions at  $k_{||} \sim 0$  with increase of excitation power. Figure 3(a) is in log-log coordinates, while Fig. 3(b) illustrates the enlarged low excitation power region with linear coordinates. The threshold of nonlinearity in the light output was clearly observed at the nominal incident power of about 90  $\mu$ W (labelled as  $T_1$ ), which indicated the onset of accumulated polariton occupation at bottom states and enhanced stimulated polariton-phonon and polariton-polariton scattering in bosonic systems. The nonlinearity

of light output was also accompanied by onset of peak blue-shift and linewidth narrowing as shown in Fig. 3(b). Narrowing of luminescence half-width represented the concentration of polaritons in the bottom states. The blue-shift of the LPB ( $\sim 1.3$  meV) was also one signature of polariton lasing, which is caused by either decreasing of exciton binding energy or the repulsive interactions among exciton-polaritons<sup>27</sup>. As further increasing the excitation power, the LPB luminescence exhibited another blue-shift to the cavity mode position of 2.973 eV. The second nonlinearity of light output and half-width narrowing at 180  $\mu$ W (labelled as  $T_2$ ) was also confirmed. This threshold was believed to be the photonic lasing.

To prospect the polariton distribution in k-space, the normalized angle-resolved PL mapping below and above the dual thresholds were recorded in Fig. 4. Below the polariton lasing threshold, the LPB emission represented a relatively uniform distribution in all angles. The polaritons condensate into the bottom states around the first threshold ( $T_1$ ). Further increasing the exciton density approaching the Mott density, the binding energy of exciton was screened by the electron-hole reservoir, resulting in the transition from strong coupling to weak coupling. By the population inversion, the luminescence in k-space would be more constricted, meanwhile the peak position blue-shifted to the cavity mode position. The phenomena observed in k-space mapping corresponded well to the nonlinearity in Fig. 3.

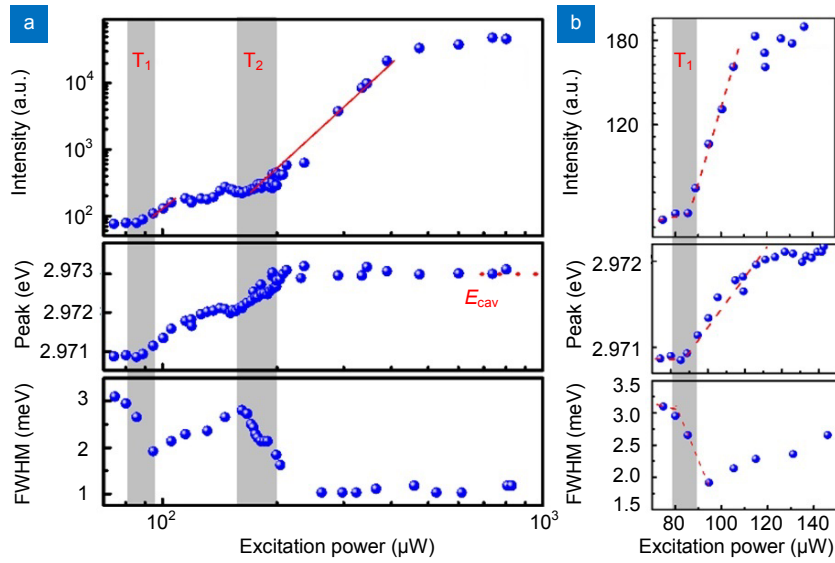


**Fig. 3 |** (a) The dependence of luminous intensity, peak position and half-width of LPB on the excitation power with double nonlinear regimes. (b) Enlarged polariton lasing region with linear coordinates. ( $T_1$  and  $T_2$  denote the polariton lasing threshold and photonic lasing threshold)

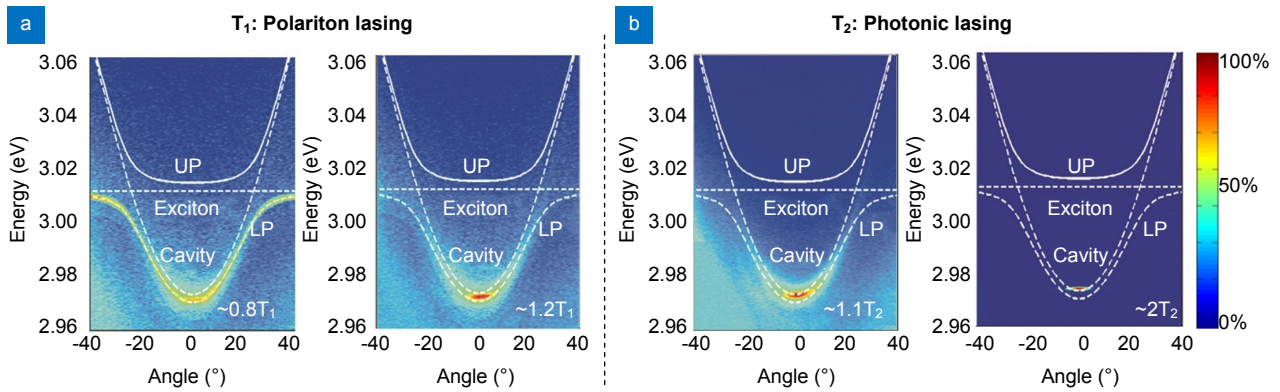


**Fig. 4 |** The k-space mapping of exciton polaritons under different excitation power. (a) and (b) polariton ( $T_1$ ) and photonic ( $T_2$ ) lasing thresholds respectively.

It is worth noting that exciton polariton lasing based on InGa<sub>N</sub> MQWs has not been reported before, due to the detrimental inhomogeneous broadening and piezoelectrical fields<sup>28</sup>. T. Tawara<sup>13</sup> and T. C. Lu<sup>14</sup> observed emission of the exciton polariton in InGa<sub>N</sub> MQWs by reflectance and electrical injection in 2004 and 2011, respectively. Although the polariton lasing in InGa<sub>N</sub> QWs was observed here in our study, the polariton lasing threshold was about half of the photonic lasing threshold. In previous reports on different materials with small exciton broadening, the polariton lasing thresholds are one or two magnitudes smaller than the photonic lasing threshold. Therefore, the polariton lasing threshold observed in our study was still higher than expected. This large polariton lasing threshold may originate from the large negative detuning value and severe exciton broadening in InGa<sub>N</sub> MQWs. As reported in Ga<sub>N</sub>/AlGa<sub>N</sub> MQWs structures, an optimum negative detuning value for the lowest polariton lasing threshold results from the

trade-off between thermodynamics and relaxation kinetics<sup>29,30</sup>. LPB with large negative detuning yields large portion of photons, which inhibits the LPB condensation and increases the polariton lasing threshold due to the reduced polariton scattering. Meanwhile, the half-width broadening of InGa<sub>N</sub> MQWs is also essential in polariton lasing action. Only those excitons whose energies match the cavity photon energy are picked out and contribute to the strong coupling and polariton lasing. Therefore, the large inhomogeneous broadening of 43 meV in our sample should also significantly increase the polariton lasing threshold.

In summary, strong coupling and polariton lasing was observed in InGa<sub>N</sub> MQWs embedded in 4.5λ microcavity at room temperature. Dual thresholds corresponding respectively to the polariton lasing and photonic lasing were clearly observed. The polariton lasing threshold was half of the photonic lasing threshold. Large negative detuning value and severe inhomogeneous



broadening of exciton in InGa<sub>N</sub> MQWs are considered to be important factors in determining the lasing threshold of polariton. Nevertheless, we believe that our work will pave a way for ultra-low threshold InGa<sub>N</sub> QWs lasers and Boson-Einstein Condensate (BEC).

## References

- Hopfield J J. Theory of the contribution of excitons to the complex dielectric constant of crystals. *Phys Rev* **112**, 1555–1567 (1958).
- Deng H, Haug H, Yamamoto Y. Exciton-polariton Bose-Einstein condensation. *Rev Mod Phys* **82**, 1489–1537 (2010).
- Deng H, Weihs G, Santori C, Bloch J, Yamamoto Y. Condensation of semiconductor microcavity exciton polaritons. *Science* **298**, 199–202 (2002).
- Kasprzak J, Richard M, Kundermann S, Baas A, Jeambrun P *et al.* Bose-Einstein condensation of exciton polaritons. *Nature* **443**, 409–414 (2006).
- Sun L X, Chen Z H, Ren Q J, Yu K, Bai L H *et al.* Direct observation of whispering gallery mode polaritons and their dispersion in a ZnO tapered microcavity. *Phys Rev Lett* **100**, 156403 (2008).
- Christopoulos S, von Högersthal G B H, Grundy A J D, Lagoudakis P G, Kavokin A V *et al.* Room-temperature polariton lasing in semiconductor microcavities. *Phys Rev Lett* **98**, 126405 (2007).
- Lai Y Y, Lan Y P, Lu T C. High-temperature polariton lasing in a strongly coupled ZnO microcavity. *Appl Phys Exp* **5**, 082801 (2012).
- Su R, Diederichs C, Wang J, Liew T C H, Zhao J X *et al.* Room-temperature polariton lasing in all-inorganic perovskite nanoplatelets. *Nano Letts* **17**, 3982–3988 (2017).
- Nakamura S. The roles of structural imperfections in InGa<sub>N</sub>-based blue light-emitting diodes and laser diodes. *Science* **281**, 955–961 (1998).
- Ponce F A, Bour D P. Nitride-based semiconductors for blue and green light-emitting devices. *Nature* **386**, 351–359 (1997).
- Nakamura S, Senoh M, Nagahama S I, Iwasa N, Yamada T *et al.* InGa<sub>N</sub>-based multi-quantum-well-structure laser diodes. *Jpn J Appl Phys* **35**, L74–L76 (1996).
- Bhattacharya P, Frost T, Deshpande S, Baten M Z, Hazari A *et al.* Room temperature electrically injected polariton laser. *Phys Rev Letts* **112**, 236802 (2014).
- Tawara T, Gotoh H, Akasaka T, Kobayashi N, Saitoh T. Cavity polaritons in InGa<sub>N</sub> microcavities at room temperature. *Phys Rev Letts* **92**, 256402 (2004).
- Lu T C, Chen J R, Lin S C, Huang S W, Wang S C *et al.* Room temperature current injection polariton light emitting diode with a hybrid microcavity. *Nano Lett* **11**, 2791–2795 (2011).
- Glauser M, Mounir C, Rossbach G, Feltn E, Carlin J F *et al.* InGa<sub>N</sub>/Ga<sub>N</sub> quantum wells for polariton laser diodes: Role of inhomogeneous broadening. *J Appl Phys* **115**, 233511 (2014).
- Christmann G, Butté R, Feltn E, Carlin J F, Grandjean N. Impact of inhomogeneous excitonic broadening on the strong exciton-photon coupling in quantum well nitride microcavities. *Phys Rev B* **73**, 153305 (2006).
- Wu J Z, Shi X L, Long H, Chen L, Ying L Y *et al.* Large Rabi splitting in InGa<sub>N</sub> quantum wells microcavity at room temperature. *Mater Res Express* **6**, 076204 (2019).
- Liu W J, Chen S Q, Hu X L, Liu Z, Zhang J Y *et al.* Low threshold lasing of Ga<sub>N</sub>-based VCSELs with sub-nanometer roughness polishing. *IEEE Photonics Technol Lett* **25**, 2014–2017 (2013).
- Liu W J, Hu X L, Ying L Y, Zhang J Y, Zhang B P. Room temperature continuous wave lasing of electrically injected Ga<sub>N</sub>-based vertical cavity surface emitting lasers. *Appl Phys Lett* **104**, 251116 (2014).
- Azuhata T, Sota T, Suzuki K, Nakamura S. Polarized Raman spectra in Ga<sub>N</sub>. *J Phys Condens Matter* **7**, L129–L133 (1995).
- Kovalev D, Averboukh B, Volm D, Meyer B K, Amano H *et al.* Free exciton emission in Ga<sub>N</sub>. *Phys Rev B* **54**, 2518–2522 (1996).
- Chichibu S, Azuhata T, Sota T, Nakamura S. Excitonic emissions from hexagonal Ga<sub>N</sub> epitaxial layers. *J Appl Phys* **79**, 2784–2786 (1996).
- Porras D, Tejedor C. Linewidth of a polariton laser: Theoretical analysis of self-interaction effects. *Phys Rev B* **67**, 161310 (2003).
- Médard F, Zuniga-Perez J, Disseix P, Mihailovic M, Leymarie J *et al.* Experimental observation of strong light-matter coupling in ZnO microcavities: Influence of large excitonic absorption. *Phys Rev B* **79**, 125302 (2009).
- Faure S, Guillet T, Lefebvre P, Bretagnon T, Gil B. Comparison of strong coupling regimes in bulk GaAs, Ga<sub>N</sub>, and ZnO semiconductor microcavities. *Phys Rev B* **78**, 235323 (2008).
- Tsintzos S I, Pelekanos N T, Konstantinidis G, Hatzopoulos Z, Savvidis P G. A GaAs polariton light-emitting diode operating near room temperature. *Nature* **453**, 372–375 (2008).
- Peyghambarian N, Gibbs H M, Jewell J L, Antonetti A, Migus A *et al.* Blue shift of the exciton resonance due to exciton-exciton interactions in a multiple-quantum-well structure. *Phys Rev Lett* **53**, 2433–2436 (1984).
- Shi X L, Long H, Wu J Z, Chen L, Ying L Y *et al.* Theoretical optimization of inhomogeneous broadening in InGa<sub>N</sub>/Ga<sub>N</sub> MQWs to polariton splitting at low temperature. *Superlattices Microstruct* **128**, 151–156 (2019).
- Butté R, Levrat J, Christmann G, Feltn E, Carlin J F *et al.* Phase diagram of a polariton laser from cryogenic to room temperature. *Phys Rev B* **80**, 233301 (2009).
- Levrat J, Butté R, Feltn E, Carlin J F, Grandjean N *et al.* Condensation phase diagram of cavity polaritons in Ga<sub>N</sub>-based microcavities: Experiment and theory. *Phys Rev B* **81**, 125305 (2010).

## Acknowledgements

This work was supported by the National Key Research and Development Program of China (No. 2016YFB0400803), the Science Challenge Project (No. TZ2016003), and the National Natural Science Foundation of China (Nos. 61704140, U1505253).

## Competing interests

The authors declare no competing financial interests.